https://doi.org/10.20965/jrm.2019.p0781

Paper:

Development of a Peristaltic-Movement Duct-Cleaning Robot for Application to Actual Environment – Examination of Brush Type and Installation Method to Improve Cleaning Efficiency –

Fumio Ito*, Takahiko Kawaguchi*, Yasuyuki Yamada, and Taro Nakamura*****

*Graduate School of Science and Engineering, Chuo University
1-13-27 Kasuga, Bunkyo-ku, Tokyo 112-8551, Japan
E-mail: {f_ito, T_Kawaguchi}@bio.mech.chuo-u.ac.jp
**Faculty of Engineering and Design, Hosei University
2-33 Ichigayatamachi, Shinjuku-ku, Tokyo 162-0843, Japan
E-mail: y.yamada@hosei.ac.jp
***Faclty of Science and Engineering, Chuo University
1-13-27 Kasuga, Bunkyo-ku, Tokyo 112-8551, Japan
E-mail: ntaro50111@gmail.com
[Received May 22, 2019; accepted October 30, 2019]

This paper describes a method to increase both the cleaning performance and speed of a peristaltic duct-cleaning robot, besides the cleaning of a real house duct. Duct piping ventilation is an important component for safeguarding indoor human health. However, dust accumulates inside such ducts during long-term use of ventilation systems. This dust leads to the generation of bacteria, dispersal of which can cause serious human health problems. Therefore, it is necessary to clean such ducts. The ducts used in factories, for example, have a large cross-sectional area and so are easy to clean by conventional duct-cleaning methods. However, as housing ducts have a small cross-sectional area and many curves, they are difficult to clean via the passive method of inserting a cleaning tool through the duct ports. For this reason, the authors attempted to develop a method of duct cleaning using a robot that imitates the peristaltic movement of earthworms. Herein, the authors examine the type and mounting position of the cleaning brush that produces the optimum cleaning efficiency. From this, we confirmed the duct cleanability of the peristaltic robot.

Keywords: peristaltic motion robot, duct cleaning robot, real house duct cleaning

1. Introduction

With the airtight nature of buildings, factories, and houses, the ventilation equipment used to exchange polluted indoor air and fresh outdoor air has become important. In many cases, pipes or "ducts" are used for ventilation, for which outdoor and indoor air is exchanged via the duct. However, dust and dirt can accumulate in the duct due to the passing of contaminated air within. This dust or dirt leads to the generation of bacteria in the duct, which can present serious human health hazards if the bacteria become scattered within the indoor environment [1, 2]. Therefore, cleaning of the inside of ducts is required.

An existing duct-cleaning method involves an operator pushing a cleaning tool, called an air lance, into the duct from one end [a]. The ducts used in large buildings, such as factories, have relatively large cross sections and few curved points; therefore, cleaning is relatively easy. Meanwhile, the ducts installed in small buildings, such as houses, have small cross-sectional areas and many curved sections. Therefore, a cleaning tool cannot be pushed all the way through the duct from one end owing to the friction or sticking that occurs in the curved sections; as a result, the deepest regions of the duct cannot be cleaned. For this reason, development of a duct cleaning robot is required.

In-pipe mobile robots have been proposed, including wheel type [3–10], ciliary vibration type [11, 12], or snake type [13–16]. However, wheel-type robots are required to be of large size to output the necessary high traction force. Moreover, snake-type robots require a large amount of space to move. Therefore, wheel-type and snake-type robots are not considered suitable for the cleaning of housing ducts with small cross-sections. In addition, the vertical and reverse movements of ciliary vibration-type robots are difficult because of their method of movement; therefore, there is a risk that such a robot cannot be removed from housing ducts with many curved sections (i.e., the robot may become trapped). Overall, it is considered that these three types of robot are not suitable for the cleaning of housing ducts.

To overcome such issues, we focused on the peristaltic movement of earthworms. Earthworms move by expand-

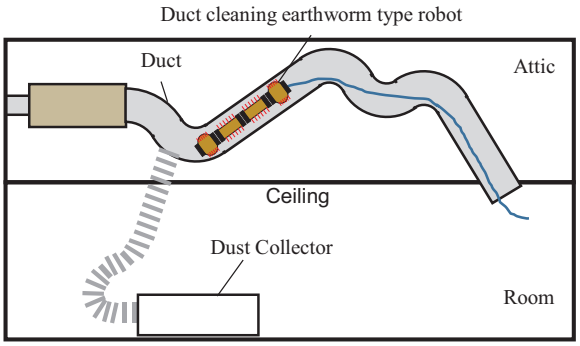

Fig. 1. Duct-cleaning robot that mimics the peristaltic movement of earthworms.

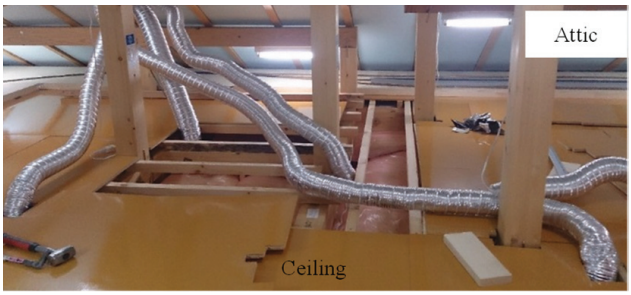

Fig. 2. Appearance of ducts installed in an attic.

ing and contracting in the axial direction, while expanding and contracting segments in the circumferential direction. Applied to a robot, this method can provide movement without requiring a large space, and allow for the grasping of the walls of a pipe of a large cross-sectional area. From this, we believe that it is possible to move a robot in a pipe with many curved sections, like in a residential duct, and a small cross-sectional area using the peristaltic motion seen in earthworms. As shown in **Fig. 1**, we developed a duct-cleaning robot that simulates the peristaltic movement of an earthworm (instead of a traditional cleaning tool) with the aim of cleaning an entire narrow residential duct with many curved sections [17].

In this paper, we discuss the structure of such a peristaltic duct-cleaning robot. Specifically, we first introduce the components of this robot. By performing cleaning experiments using the robot, we investigated different types of cleaning brushes to enhance the cleaning performance. We also examined the installation of the cleaning brush to improve both the cleaning performance and cleaning speed. Finally, the feasibility of the robot was examined via an experiment on a duct installed in a real house.

2. Current Status of Housing Duct Cleaning

2.1. Duct Installation in Houses

Figure 2 shows the appearance of ducts installed in a real house. As shown in **Fig. 3(a)**, most ducts installed in the house had an inner diameter of approximately 50 mm,

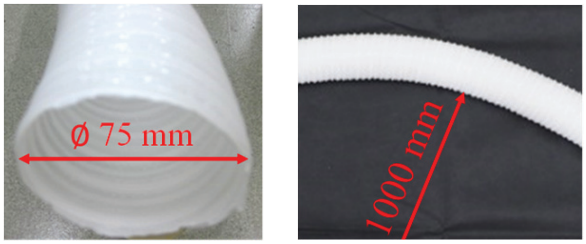

(a) (b)

Fig. 3. (a) Inner diameter and (b) radius of curvature of duct.

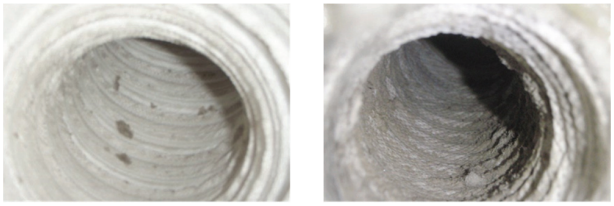

(a) (b)

Fig. 4. Contamination (a) before and (b) after long-term use of a duct.

although there were also many ducts with an inner diameter of 75 mm. As such, the ducts had small cross-sectional areas, as well as internal irregularities. Furthermore, to save space in the installation area, the ducts were installed using many curves with a radius of curvature of approximately 1 m, as shown in **Fig. 3(b)**. In a typical house, approximately eight to ten ducts are installed, with a maximum length of $\sim$10 m. The indoor space and outdoor space are connected via these ducts and ventilation occurs by the exchange of air. However, as shown in **Fig. 4**, dust and dirt can collect inside the ducts over time. Accumulated dust adheres to the duct walls via static electricity and moisture. Bacteria may then be generated in the dust and dirt, and may be released into the rooms of the house, leading to human health damage. Therefore, the inside of the ducts should be cleaned regularly.

2.2. Existing Duct-Cleaning Method

In this section, the typical duct cleaning method is explained. As described in Section 2.1, dust adheres to the duct walls, necessitating their cleaning. A cleaning tool called an air lance (**Fig. 5**) is used for this purpose. The air lance is inserted into a duct from one end. An air tube is then connected to the rear of the air lance and the lance is pushed to the end of the duct. When air is supplied to the air tube in this state, the air lance at the tip is activated and removes dust from the inner wall of the duct. The dust removed is then picked up by a dust collector. In this cleaning method, the air lance is pushed into the duct only by the force of the operator's hand; therefore, the friction generated in curved sections may prevent cleaning beyond the curve. Furthermore, cleaning with this method requires approximately 3–4 h per house, which is a relatively long time. If the shape of the duct is com-

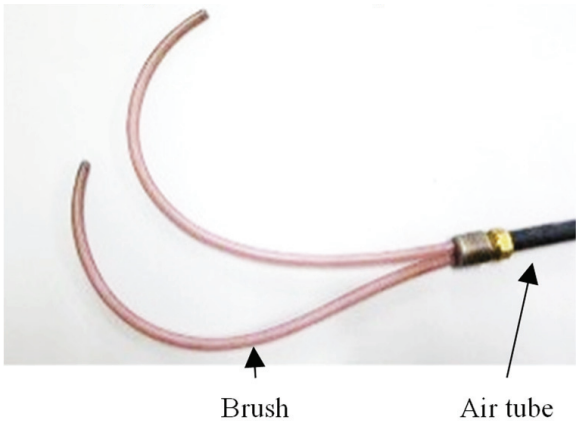

Fig. 5. Duct-cleaning tool (air lance).

plicated and difficult to clean, it is necessary to replace the duct, which requires removal of the ceiling and is costly. Therefore, cleaning by a self-propelled robot offers many potential advantages.

2.3. Required Specifications of Duct-Cleaning Robot

As it is difficult to clean the inside of a duct with many thin curved sections using the existing cleaning method, we propose that such cleaning is conducted using a self-propelled robot. The duct-cleaning robot should satisfy the following criteria to account for the installation and cleaning conditions.

- Move and clean inside a duct with an inner diameter of 50 or 75 mm.
- Move and clean in a 10-m-long duct.
- Move and clean at a minimum speed of 16.7 mm/s.

3. Outline of a Peristaltic Robot for Duct Cleaning

3.1. Earthworm Peristaltic Movement

The structure of an earthworm comprises the connection of a plurality of segments with the same structure. **Fig. 6** demonstrates the movement of an earthworm. The worm first contracts the segments of the head in the axial direction. Next, the axial contraction is propagated to the posterior segments and extended in the axial direction sequentially from the leading segment. When axial contraction propagates to the tail segment, axial contraction is repeated from the head. The axially shrunken segments expand circumferentially and generate friction. The earthworm progresses using this friction.

In this movement method, the space required for movement is small. Based on this method of movement, robots capable of travelling over long distances in small-diameter pipes have been developed [18, 19]. Stable travelling over long distances is possible as a pipe wall can be grasped over a large area.

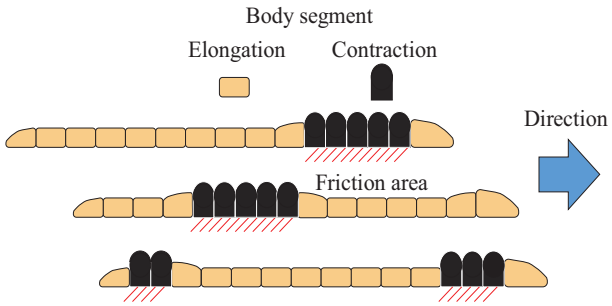

Fig. 6. Schematic of peristaltic movement of an earthworm.

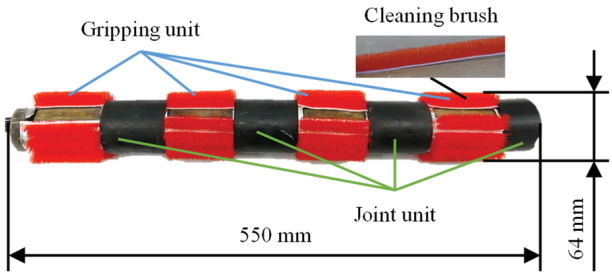

Fig. 7. Appearance of peristaltic robot for duct cleaning.

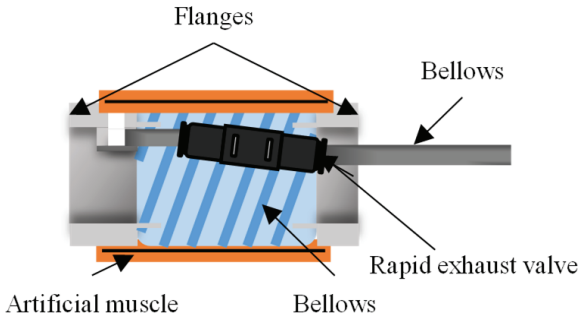

Fig. 8. Unit structure of duct-cleaning robot.

3.2. Peristaltic Robot for Duct Cleaning

An overview of the duct-cleaning robot is shown in **Fig. 7**. This robot was configured by connecting four gripping units with three joint units. By driving each gripping unit in order from the lead gripping unit, the robot could advance in a duct with an inner diameter of 75 mm owing to its peristaltic motion. Furthermore, the cleaning brush attached to the robot could clean by contacting the inner wall of the duct during travel. It was possible to check the cleanliness inside the duct using an endoscope attached to the head of the robot.

3.3. Structure of Gripping Unit

Figure 8 shows the structure of the gripping unit. This gripping unit comprises two flanges, bellows, a rapid exhaust valve (PISCO EQU-6), and an axial fiber-reinforced

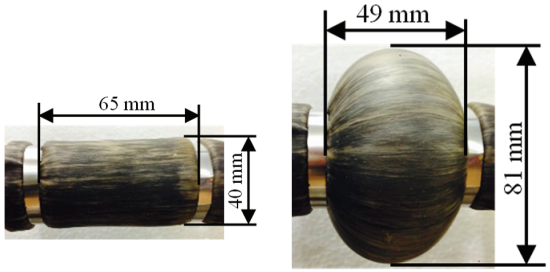

Fig. 9. (a) Relaxation and (b) contraction of the gripping unit.

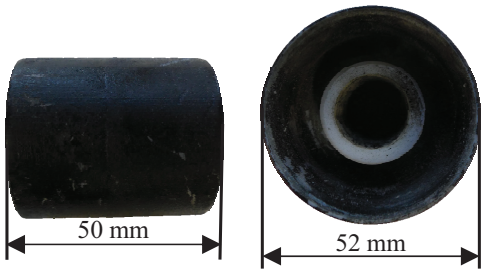

Fig. 10. (a) Side and (b) front views of joint unit of peristaltic duct-cleaning robot.

artificial muscle [20, 21]. As shown in **Fig. 9**, when air pressure was applied in the chamber of this gripping unit, the gripping unit contracted in the axial direction and expanded in the radial direction. The rapid exhaust valve reduced the air exhaust time of the gripping unit.

3.4. Structure of Joint Unit

Figures 10(a) and **(b)** show the side and front of a joint unit, respectively. This joint unit could be connected to the gripping unit in a removable manner. As such, the number and type of gripping units could be adjusted according to the traveling environment. In addition, the radius of the joint unit was made larger than the radius of the gripping unit because the rubber tube used for the artificial muscle was considered to exhibit a high degree of friction with the pipe wall. Therefore, the rubber tube could travel without touching the inner wall of the duct.

3.5. Cleaning Brush

Three brushes were tested to determine which exhibited the best cleaning performance.

The dust in the duct is peeled off by the friction generated by the cleaning brush rubbing the inner wall of the duct. Therefore, the type of cleaning brush has a direct effect on the cleaning performance. However, brushes are not regulated according to a clear standard. In this study, we used brushes with different hardness and lengths, as shown in **Figs. 11**–**13**. In addition, these hardness and lengths are according to each specific application of the brushes tested: super crimped piles (**Fig. 11**; hereinafter, "cleaning brush 1") are used for carpets on the floor, mop

Fig. 11. Super crimped pile.

Fig. 12. Mop brush.

Fig. 13. Nylon brush.

Table 1. Characteristics of each cleaning brush.

	Length [mm]	Hardness	Material
Super-crimped pile	7	Soft	Nylon
Mop brush	11	Soft	Cotton
Nylon brush	11	Hard	Nylon

brushes (**Fig. 12**; hereinafter, "cleaning brush 2") are used for floor cleaning, and nylon brushes (**Fig. 13**; hereinafter, "cleaning brush 3") are used to silence the door opening and closing sounds because they have elasticity.

Table 1 shows the length and hardness of each cleaning brush.

3.6. Cleaning Brush Installation Method

By winding the cleaning brush around the gripping unit and joint unit, as shown in **Figs. 14** and **15**, the cleaning brush contacted and cleaned the inner wall of the duct as the robot traveled through the duct. To prevent the cleaning brush from interfering with the expansion in the circumferential direction of the gripping unit, the cleaning brush was attached to an aluminum deposition sheet with an axial notch to produce a brush sheet, as shown in **Fig. 16**. This brush sheet was wrapped around the gripping unit and fixed with tape. When attached to the joint unit, the brush sheet (**Fig. 17**) was wound in the circumferential direction.

3.7. Cleaning Brush Mounting Position

Three mounting positions (A, B, and N; **Fig. 18**) were examined for the cleaning brush. For type A, the cleaning brush was attached to the gripping unit. For type B, the

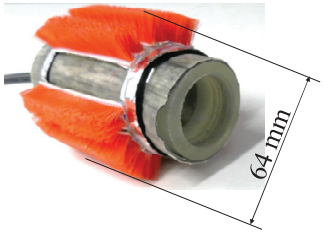

Fig. 14. Gripping unit with cleaning brush attached.

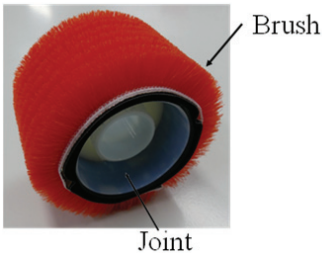

Fig. 15. Joint unit with cleaning brush attached.

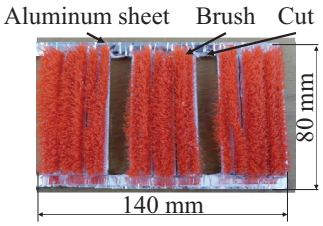

Fig. 16. Cleaning brush sheet attached to the gripping unit.

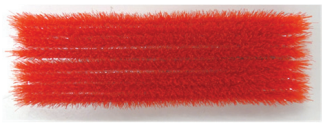

Fig. 17. Cleaning brush sheet attached to the joint unit.

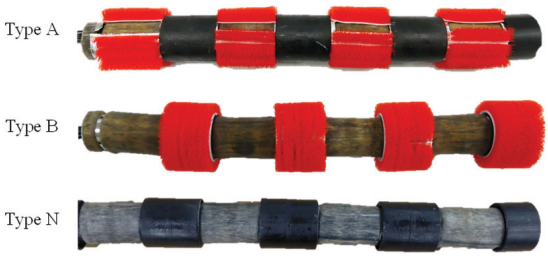

Fig. 18. Attachment of cleaning brush to peristaltic robot for duct cleaning.

cleaning brush was attached to the joint unit. Meanwhile, type N did not have an attached cleaning brush.

Figure 19 shows the principle of each type of cleaning. When the robot moves inside the duct, the outer peripheral surface of the robot rubs against the duct inner wall. As a result, it is possible to rub off dust stuck to the inner wall of the duct. For type A, the brush moves relative to the

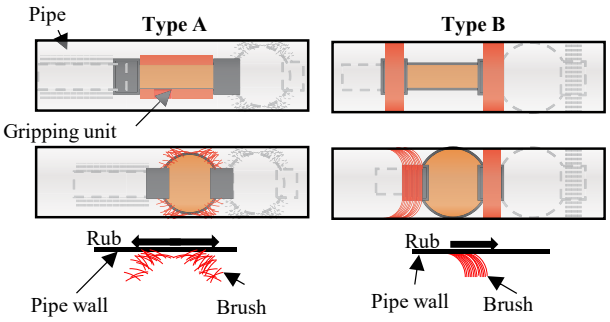

Fig. 19. Cleaning principles for type A and B robots.

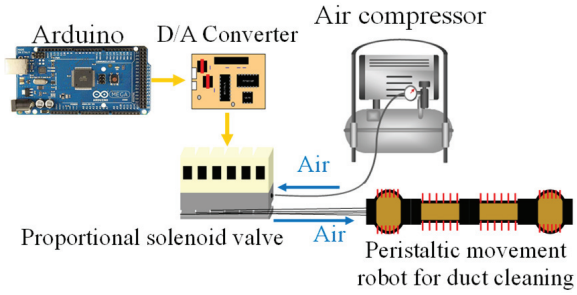

Fig. 20. Control system of peristaltic robot for duct cleaning.

inner wall of the duct as the gripping unit contracts and extends. From this, it can be expected that type A can efficiently convert the expansion capacity of the gripping unit into cleaning capacity. Meanwhile, as type B runs in the pipe, the brush continuously rubs against the duct. From this, it is considered that the running capacity can be efficiently converted to the cleaning ability.

3.8. Earthworm Robot Control System for Duct Cleaning

Figure 20 shows the control system of a peristaltic robot for duct cleaning. The air pressure applied to each segment was controlled by an Arduino Mega 2560. The D/A converter converted the digital voltage from the Arduino into an analog voltage, which was then sent to a proportional solenoid valve. The air pressure of the compressor was applied to each segment via a manifold and a proportional solenoid valve. As a result, each gripping unit could expand and contract independently.

3.9. Operation Pattern of the Earthworm Robot for Duct Cleaning

The operation pattern of the robot is shown in **Fig. 21**. As can be seen, by applying air pressure to the gripping units in order (from the front) in the direction of travel, the robot could travel using peristaltic motion, like an earthworm. Furthermore, it was possible to induce backward movement by applying air pressure to the gripping units in the reverse order.

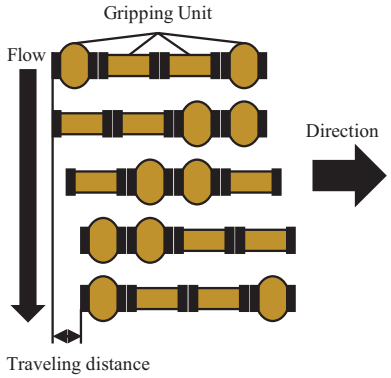

Fig. 21. Motion pattern of peristaltic robot for duct cleaning.

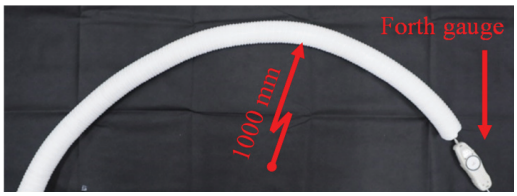

Fig. 22. Environment for measuring the necessary traction of peristaltic robot for duct cleaning.

4. Required Traction of Robot

In this paper, we aimed to clean a 50-mm inner diameter duct, which is the most common size of ducts in real houses. We produced a trial peristaltic robot with an inside diameter of 75 mm, which was relatively easy to manufacture, and determined the specifications of the robot.

This robot was required to tow a 10-m air tube as well as the rear gripping unit and joint unit. Therefore, we measured the tractive force required when the robot traveled in a duct with an inner diameter of 75 mm and length of 10 m, as installed in a general residence.

The conditions of the measurement are shown in **Fig. 22**. The robot and air tube were placed in a duct with a radius of curvature of 1 m. Using a force gage, the static frictional force of the robot and air tube placed in the duct was measured as 72 N. From this, the necessary pulling force was considered to be 72 N, and a gripping unit was developed that exceeded this pulling force.

5. Examination of Type of Cleaning Brush

In this section, using a type-A duct-cleaning peristaltic robot, we consider the different cleaning brushes in terms of their cleaning performance. **Fig. 23** shows the appearance of the gripping unit with the cleaning brushes attached. The gripping unit attached with cleaning brush 1 (**Fig. 23(a)**) is termed gripping unit 1. The gripping unit attached with cleaning brush 2 (**Fig. 23(b)**) is termed gripping unit 2, and the gripping unit attached with cleaning brush 3 (**Fig. 23(c)**) is termed gripping unit 3.

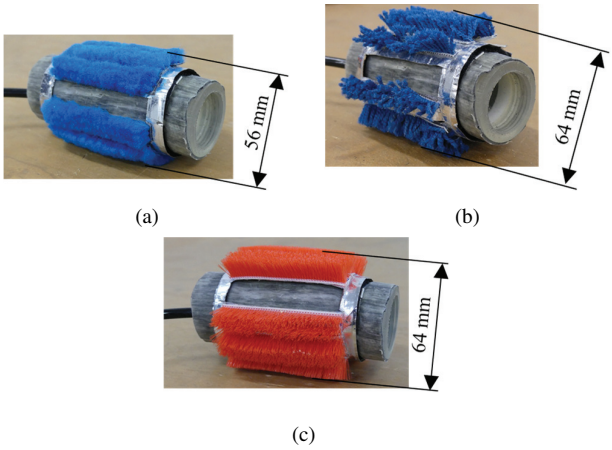

Fig. 23. Images of the gripping unit attached with (a) super crimped pile brush, (b) mop brush, and (c) nylon brush.

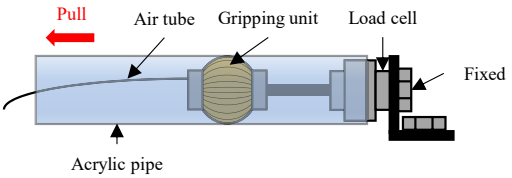

Fig. 24. Experimental environment for measuring the gripping force of gripping units equipped with each cleaning brush.

5.1. Gripping Force Measurement Experiment

In this section, the gripping force of the gripping unit is considered. As mentioned in Section 2.1, the duct had an inner helical asperity. Meanwhile, acrylic pipes are smooth, without inner unevenness. Therefore, compared with the case where the gripping unit grips an acrylic pipe, the gripping unit can become caught on the unevenness of the inner surface of the duct, and a larger gripping force can be generated. Therefore, it is considered that a gripping unit that generates a gripping force of 72 N or more in an acrylic pipe can also generate a gripping force of 72 N or more in a duct. Using a transparent acrylic pipe that allowed visual confirmation of the gripping unit gripping the inside of the pipe, the gripping force of the gripping unit with each cleaning brush attached was measured. For comparison, we also measured the gripping force of the gripping unit without an attached cleaning brush.

The experimental environment is shown in **Fig. 24**. The gripping unit was placed in an acrylic pipe (inner diameter of 75 mm) and then pressure was applied to the gripping unit to induce gripping of the pipe. In this state, the pipe was pulled, and the gripping force when the gripping unit slipped was measured by the load cell as the maximum gripping force. The applied pressure was increased from 0.10 MPa in steps of 0.01 MPa, and the lowest pressure at which the gripping force reached 72 N or more was determined. In addition, it was confirmed in advance that the gripping force exceeded 72 N when 0.10 MPa

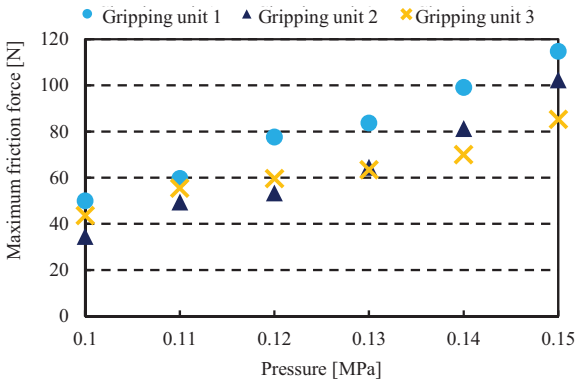

Fig. 25. Gripping force measurement results for each gripping unit.

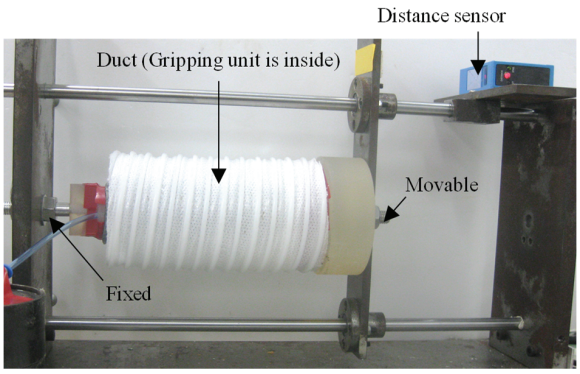

Fig. 26. Contraction response measurement environment of gripping unit with each cleaning brush attached.

Table 2. Contraction response measurement results of the gripping unit with each cleaning brush attached.

	Contraction time [s]	Elongation time [s]	Amount of contraction [mm]
Non-pile	0.60	0.60	16.0
Unit 1	0.90	0.60	14.0
Unit 2	0.83	0.66	15.7
Unit 3	0.87	0.63	15.9

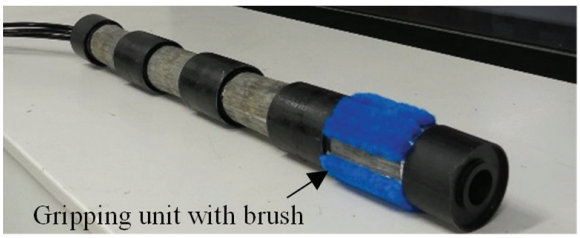

Fig. 27. Robot with brush attached only at the top.

was applied to the gripping unit without a cleaning brush attached.

The experimental results are shown in **Fig. 25**. The maximum static frictional force exceeded 72 N when an air pressure of 0.12 MPa was applied to the gripping unit 1, 0.14 MPa to gripping unit 2, and 0.15 MPa to gripping unit 3. The gripping unit without an attached cleaning brush had a gripping force of 72 N at 0.10 MPa. As described above, in the case of the holding unit without a cleaning brush, a large holding force was generated, even at low pressure. This is considered to be because the frictional force generated by the rubber tube used for the artificial muscle was larger than the frictional force generated by the cleaning brush.

It can be seen that the maximum frictional force of the gripping unit increased in the following order: gripping unit 1, gripping unit 2, gripping unit 3. This may be because the cleaning brush was short and the softer one in close contact with the cleaning brush and the duct.

Based on these experimental results, an applied pressure of 0.15 MPa, which exceeds the gripping force of 72 N, was adopted in all gripping units in the following brushed units.

5.2. Measurement of Elongation and Contraction Time

In this section, the contraction and elongation responses of the gripping unit are considered. The experimental environment is shown in **Fig. 26**. A gripping unit with each cleaning brush installed was placed in the duct with one end fixed. In this state, air pressure was applied to the gripping unit and the displacement of the movable component was measured with a laser displacement meter when the gripping unit was contracted and extended. The applied pressure was 0.15 MPa, the length of the air tube was 10 m, and the inside diameter of the air tube was 4 mm.

Table 2 shows the experimental results. With a cleaning brush attached to the gripping unit, the contraction time increased and the amount of contraction decreased, compared with the gripping unit without a cleaning brush attached. This is considered to be because the amount of expansion of the gripping unit was reduced by the cleaning brush. In addition, the hardness and length of each brush hinder the contraction and expansion of the artificial muscle, which may affect the contraction time.

Moreover, from the results of these experiments, the contraction time and extension time of the gripping unit with an attached cleaning brush were 0.90 s and 0.60 s, respectively. The contraction time and extension time of the gripping unit without a cleaning brush attached were 0.60 s and 0.60 s, respectively.

5.3. Cleaning Experiment for Cleaning Brush Decision

In this section, we consider the types of cleaning brushes regarding the cleaning performance. To examine only the influence of the brush type on the cleaning performance, a cleaning experiment was conducted by a robot in which the cleaning brush was attached only to the leading gripping unit, as shown in **Fig. 27**. For comparison, cleaning was also performed using a robot without a cleaning brush. In addition, the pipe to be cleaned was a

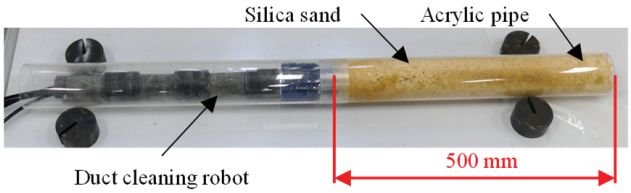

Fig. 28. Experimental environment for determining the most efficient type of cleaning brush.

Table 3. Parameters for calculating the cleaning rate.

E [%]	Cleaning rate
m [g]	Mass to be cleaned before cleaning
M [g]	Mass to be cleaned after cleaning

transparent acrylic pipe, the inside of which could be easily checked to confirm that the robot was able to clean the entire pipe evenly.

The experimental environment is shown in **Fig. 28**. A test powder (silica sand) was adhered to the inside of the transparent acrylic pipe (inner diameter: 75 mm, length: 500 mm) according to the following procedure.

i. An atomizer was used to wet the inside of the acrylic pipe with water.

ii. With one end of the acrylic pipe closed, 50 g of test powder was placed in the pipe and attached evenly throughout the entire pipe.

iii. To ensure that the test powder was firmly adhered to the inside of the acrylic pipe, the pipe was wetted again using atomization.

The weight of the test powder in the duct was determined by measuring the weight of the duct with the test powder attached and the weight of the duct with no test powder attached. The degree of cleaning was compared after each robot traveled through the pipe with the test powder adhered. Eq. (1) was used for the evaluation. **Table 3** shows the parameters used in Eq. (1). This equation presents the ratio between the masses of the test powder in the acrylic pipe before and after cleaning.

$$E = \left(1 - \frac{M}{m}\right) \times 100. \quad \ldots\ldots\ldots\ldots (1)$$

The condition after cleaning is shown in **Fig. 29**. Additionally, **Fig. 30** shows the weight and cleaning rate of the removed powder. From this, it can be seen that the cleaning rate followed the order: gripping unit 1 < gripping unit 2 < gripping unit 3. This indicates that the cleaning rate was higher when the cleaning brush was hard. This is considered to be because if the cleaning brush was soft, the robot would push dust against the pipe wall, making it difficult to clean. Furthermore, the longer the cleaning brush, the better the cleaning rate tended to be. This is considered to be because the longer the cleaning brush, the longer the contact time between the pipe wall and the

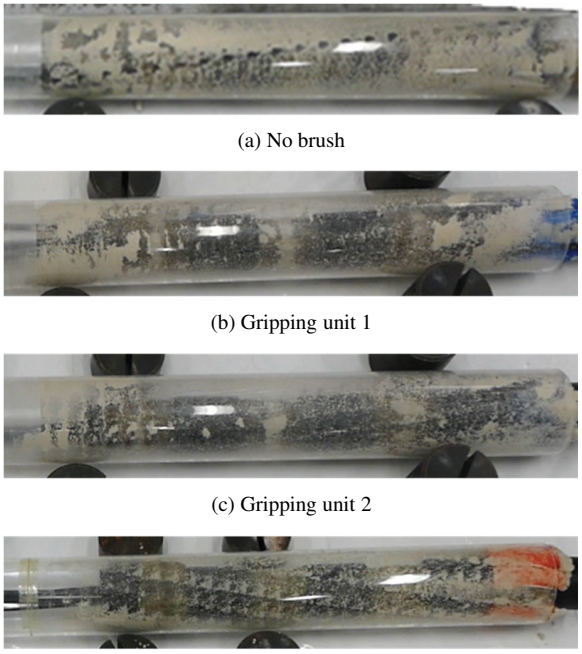

(a) No brush

(b) Gripping unit 1

(c) Gripping unit 2

(d) Gripping unit 3

Fig. 29. Cleaning experiment environment to determine the most efficient type of cleaning brush.

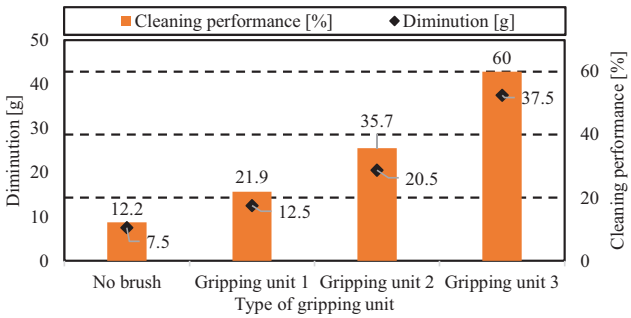

Fig. 30. Cleaning test results and cleaning rates to determine the most efficient type of cleaning brush.

cleaning brush per cycle. As shown in **Fig. 28**, there were spots in the cleaning, as can be seen from the state of the test powder in the tube after cleaning. From this, it seems that the cleaning situation becomes uneven with a single brush.

Based on these experimental results, we used the nylon brush with the highest cleaning performance as the cleaning brush in future experiments.

6. Examination of Cleaning Brush Installation Position

In this section, we consider the installation position of the cleaning brush. The purpose of this robot is to clean ducts. When cleaning housing ducts, a limited amount of time is generally available to complete the cleaning; therefore, cleaning speed is important. From this, we

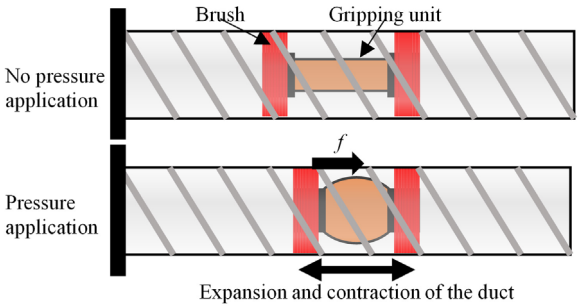

Fig. 31. Expansion and contraction of duct due to the brush movement.

aimed to identify the cleaning brush installation position that could increase the traveling speed while maintaining a high cleaning rate. The cleaning brush used was the nylon brush as it exhibited the highest cleaning performance in Section 5.3.

6.1. Cleaning Brush Mounting Position Determination

Here, we consider types A and B cleaning brush mounting positions. For the type-A robot, the cleaning brush periodically contacted the inner wall of the duct. Meanwhile, the brush of a type-B robot continuously contacts the inner wall of the duct, so the duct expands and contracts due to the friction generated on the inner wall of the duct, as shown in **Fig. 31**. Based on this, it was considered that the cleaning performance of type-B robots was significantly affected by the brush length, and the experiment was performed for different brush lengths. As such, for type-B robots, we also consider the cleaning brush length. Moreover, the joint units with a cleaning brush attached with diameters of 73 mm (B-1), 75 mm (B-2), and 77 mm (B-3) were considered. For comparison, we also conducted cleaning experiments with type-N robots. From **Table 2** in Section 5.2, the contraction time and extension time for type A are 0.90 s and 0.60 s, respectively, and those for type N are 0.60 s and 0.60 s, respectively.

6.2. Driving Experiment with Changes in Cleaning Brush Position

In this section, the running speed of each robot is compared. The average velocity of each robot traveling in a duct (inner diameter 75 mm, length 50 mm) was measured.

The experimental results are shown in **Fig. 32**. In terms of the traveling speed, type B was faster than type A. This is thought to be because the expansion of the artificial muscle in type B was not impeded by the thickness of the cleaning brush, and contraction of the artificial muscle efficiently led to axial contraction. In addition, type-B robots operated faster with shorter cleaning brushes. This is considered to be because the longer the cleaning brush, the greater the force with which it was pressed against the pipe wall, increasing the travel resistance.

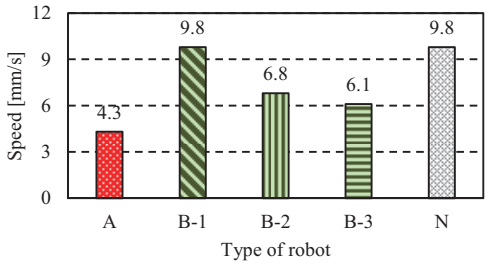

Fig. 32. Influence of cleaning brush mounting position on traveling speed.

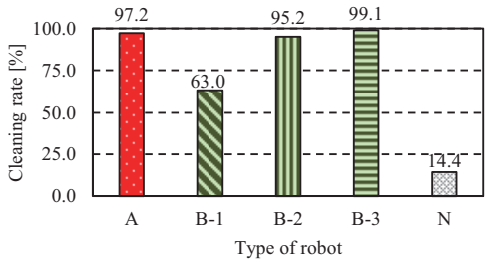

Fig. 33. Influence of cleaning brush mounting position on cleaning rate.

6.3. Cleaning Experiment with Cleaning Brush Position Changes

In this section, we consider the cleaning experiments conducted with each robot and examine the effect of the cleaning brush installation position on the cleaning efficiency. The experimental method was the same as that shown in **Fig. 28** in Section 5.3. However, to conduct the experiments in a more realistic environment, an actual duct was used as the running pipe.

The experimental results are shown in **Fig. 33**. **Figs. 34** and **35** show the conditions before and after cleaning with type A and type B-3, respectively. Type A had a cleaning rate of 97.2%, whereas type B had a maximum cleaning rate of 99.1% when the joint unit diameter was 77 mm. From this, it is considered that type B exhibits a better traveling speed and cleaning rate than those of type A. In addition, it is thought that the cleaning rate will actually be higher because a dust collector is used in conjunction with the robot.

From these findings, it is considered that the robot can travel through a duct while maintaining a sufficient cleaning rate. In the next section, the robot is improved based on real-world conditions, and ducts installed in a house are cleaned.

7. Real House Duct Cleaning Experiment

7.1. Duct-Cleaning Robot for Real House-Duct Cleaning

The detailed design of the robot was changed based on a real-world environment. **Fig. 36** shows the redesigned

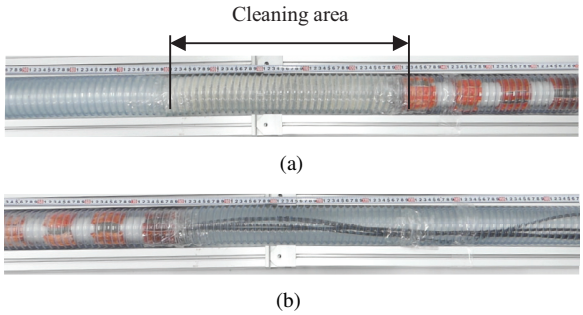

Fig. 34. Ducts (a) before and (b) after cleaning with type A.

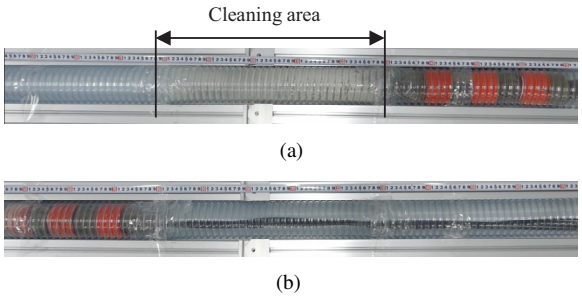

Fig. 35. Ducts (a) before and (b) after cleaning with type B.

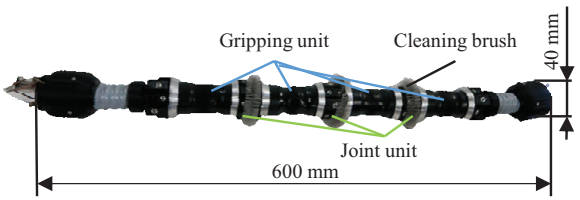

Fig. 36. Peristaltic robot used for cleaning a real house duct.

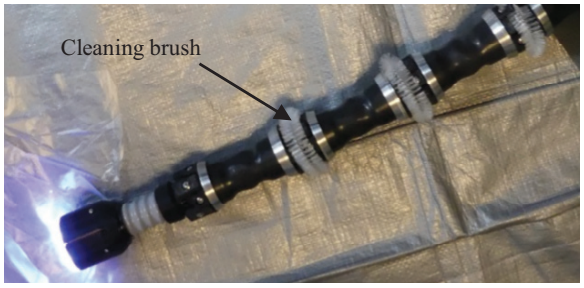

Fig. 37. Cleaning brush image of peristaltic robot for cleaning a real house duct.

robot. As shown in **Fig. 37**, the nylon brush (which showed the best cleaning rate in the cleaning test [Section 5.3]) was wound around the joint unit of the robot. The purpose of this robot was to clean the inside of a duct with an inner diameter of 50 mm. The basic structure was the same as that of the type-B robot. Because the interior of an actual residential duct is dark, it was necessary to add illumination to check the cleaning status. Therefore, an LED light, as shown in **Fig. 38**, was attached to the top of the robot. This made it possible to check the internal condition using an endoscope while the robot moved through the duct. The control box, shown in **Fig. 39**, controlled the air pressure applied to the robot, as well as the timing of its application. This control box was equipped with a monitor that captured endoscopic images. By placing these in a single box, transportation was eased.

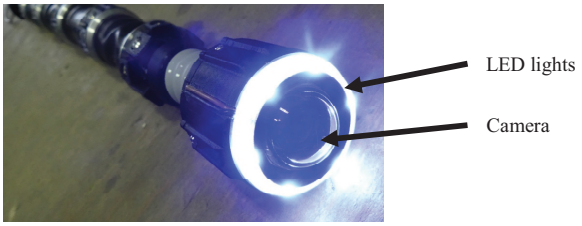

Fig. 38. Image of the top of peristaltic robot for cleaning a real house duct.

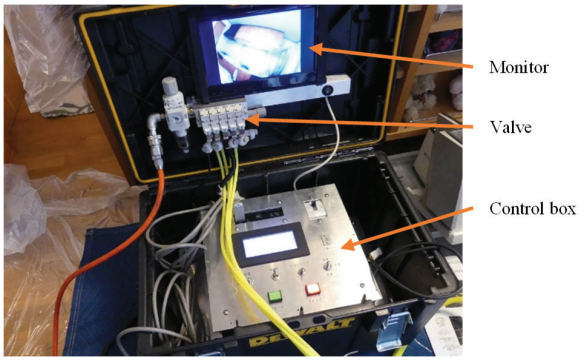

Fig. 39. Control box and endoscope monitor of peristaltic robot for cleaning a real house duct.

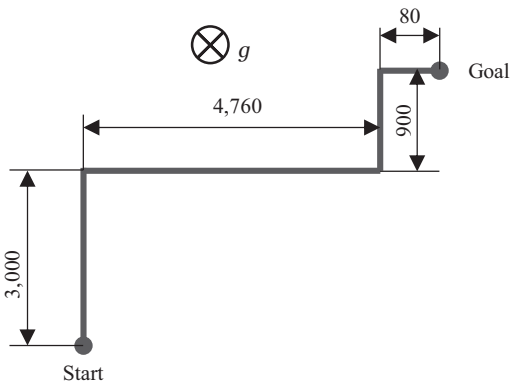

Fig. 40. Real-house duct-cleaning course 1.

7.2. Cleaning Duct Pipeline

The robot was used to clean the ducts installed in a real house. Outlines of the courses run are shown in **Figs. 40–42** (all units are in mm). The courses are numbered 1 to 3 below. The outline of a course was based on the installation drawing of the duct; the radius of curvature of the duct was approximately 1 m.

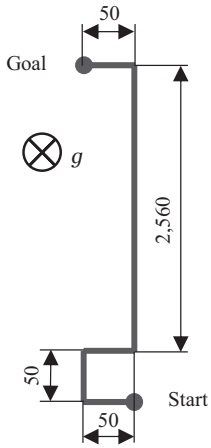

Fig. 41. Real-house duct-cleaning course 2.

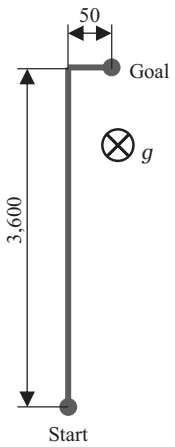

Fig. 42. Real-house duct-cleaning course 3.

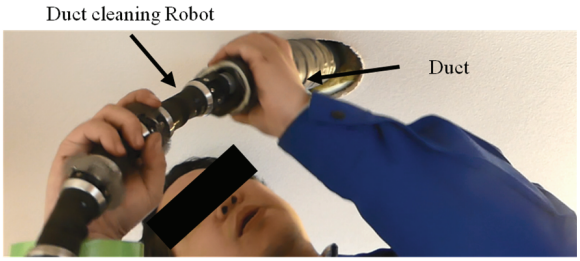

Fig. 43. State of actual house cleaning with duct-cleaning robot.

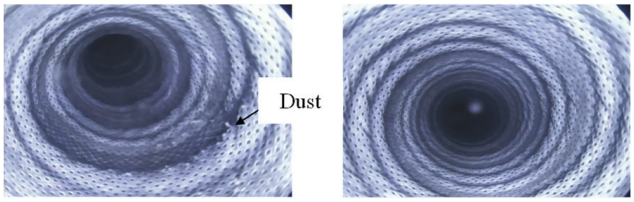

Fig. 44. Inside the duct before and after actual house cleaning with the duct-cleaning robot.

7.3. Driving Situation

In course 1, in addition to the bend in the horizontal plane shown in the drawing, there were many curved sections in the vertical direction. It took approximately 1 h to run the course. In course 2, a decrease in the speed was observed at the curve at the end of the course; therefore, cleaning of course 2 took approximately 30 min. In course 3, cleaning was completed in approximately 40 min.

7.4. Duct Cleaning Condition

Figure 43 shows the cleaning during the experiment in an actual house. Cleaning of the duct used the same process as the air lance method described in Section 2.2. However, the work performed by the air lance was instead performed by the robot.

Figure 44 shows the images obtained by the endoscope attached to the robot before and after cleaning, respectively. Before cleaning, dirt such as paper dust was present in the duct, whereas after cleaning, the paper dust in the duct was removed.

Fig. 45. Condition of the peristaltic duct cleaning robot after actual house cleaning.

The appearance of the robot after cleaning is shown in **Fig. 45**; the robot was dirty and would need to be cleaned before its next use. Furthermore, the endoscope may be contaminated and so its images may not be clear. In the future, we would like to develop a structure that prevents dust collection on the endoscope on the top of the robot.

The robot traveled through the duct installed in a house and cleaned it effectively. From this, we consider that the peristaltic duct-cleaning robot is practicable. However, the cleaning time was 30–60 min per duct; in the future, we would like to consider ways to further increase the cleaning efficiency.

8. Conclusion

In this paper, we examined the structure and cleaning efficiency of a peristaltic robot for duct cleaning through experimental studies. From experiments conducted in the laboratory, it was confirmed that the robot could clean the inside of a duct with a cleaning rate of 99.1%. Furthermore, the design of the robot was adapted to better suit real-world situations, and it was used through the ducts of three real houses to determine its cleaning capabilities. The robot performed efficient duct cleaning in all cases, confirming its applicability to real-world conditions.

In the future, we would like to conduct a quantitative evaluation of the cleaning efficiency in field experiments. Furthermore, we aim to improve the cleaning speed by performing pressure control and design changes.

Acknowledgements

We gratefully acknowledge Tokyo Metropolitan Industrial Technology Research Institute for their financial support. The authors also thank Nippon Winton Co., Ltd. for technical assistance with the experiments.

References:
[1] B. Zhou, B. Zhao, and Z. Ta, "How Particle Resuspension from Inner Surfaces of Ventilation Ducts Affects Indoor Air Quality – A Modeling Analysis," Aerosol Science and Technology, Vol.45, No.8, pp. 996-1009, 2011.
[2] H. Yoshino, K. Amano, M. Matsumoto, K. Netsu, K. Ikeda, A. Nozaki, K. Kakuta, S. Hojo, and S. Ishikawa, "Long-termed Field Survey of Indoor Air Quality and Health Hazards in Sick House," J. of Asian Architecture and Building Engineering, Vol.3, No.2, pp. 297-303, 2004.
[3] H. M. Kim, Y. S. Choi, Y. G. Lee, and H. R. Choi, "Novel Mechanism for In-Pipe Robot Based on a Multiaxial Differential Gear Mechanism," IEEE/ASME Trans. on Mechatronics, Vol.22, Issue 1, pp. 227-235, 2017.
[4] A. Kakogawa, Y. Oka, and S. Ma, "Multi-link Articulated Wheeled In-pipe Robot with Underactuated Twisting Joints," Proc. of 2018 IEEE Int. Conf. on Mechatronics and Automation, August 5-8, Changchun, China, pp. 942-947, 2018.
[5] T. Nishimura, A. Kakogawa, and S. Ma, "Improvement of a Screw Drive In-Pipe Robot with Pathway Selection Mechanism to Pass through T-Branches," J. Robot. Mechatron., Vol.25, No.2, pp. 340-346, 2013.
[6] H. Amir, M. Heidari, R. Mehrandezh et al., "Dynamic analysis and human analogous control of a pipe crawling robot," Proc. of IEEE/RSJ Int. Conf. on Intelligent Robots and Systems 2009, October 10-15, Missouri (TX), St. Louis, pp. 733-740, 2009.
[7] Y.-S. Kwon, B. Lee, I.-C. Whang, W.-K. Kim, and B.-J. Yi, "A Flat Pipeline Inspection Robot with Two Wheel Chains," 2011 IEEE Int. Conf. on Robotics and Automation, pp. 5141-5146, 2011.
[8] H.-O. Lim and T. Ohki, "Development of Pipe Inspection robot," Proc. of ICROS-SICE Int. Joint Conf., pp. 5717-5721, 2009.
[9] S. U. Yang, H. M. Kim, J. S. Suh, Y. S. Choi, H. M. Mun, C. M. Park, H. Moon, and H. R. Choi, "Novel Robot Mechanism Capable of 3D Differential Driving Inside Pipelines," 2014 IEEE/RSJ Int. Conf. on Intelligent Robots and Systems (IROS 2014), September 14-18, Chicago, IL, USA, pp. 1944-1949, 2014.
[10] H. M. Kim, Y. S. Choi, Y. G. Lee, and H. R. Choi, "Novel Mechanism for In-Pipe Robot Based on a Multiaxial Differential Gear Mechanism," IEEE/ASME Trans. on Mechatronics, Vol.22, No.1, pp. 227-235, 2017.
[11] M. Konyo, K. Hatazaki, K. Isaki, and S. Tadokoro, "Development of an active scope camera driven by ciliary vibration mechanism," Proc. of the 12th ROBOTICS Symposia, March 15-16, Nagaoka, pp. 460-465, 2007.
[12] M. Konyo, K. Isaki, K. Hatazaki, S. Tadokoro, and F. Takemura, "Ciliary Vibration Drive mechanism for Active Scope Cameras," J. Robot. Mechatron., Vol.20, No.3, pp. 490-499, 2008.
[13] S. Xiao, Z. Bing, K. Huang, and Y. Huang, "Snake-like Robot Climbs Inside Different Pipes," Proc. of 2017 IEEE Int. Conf. on Robotics and Biomimetics (ROBIO), pp. 1232-1239, 2017.
[14] E. Prada, M. Valášek, I. Virgala, A. Gmiterko, M. Kelemen, M. Hagara, and T. Lipták, "New Approach of Fixation Possibilities Investigation for Snake Robot in the Pipe," Proc. of 2015 IEEE Int. Conf. on Mechatronics and Automation (ICMA), pp. 1204-1210, 2015.
[15] F. Trebuňa, I. Virgala, M. Pástor, T. Lipták, and L. Miková, "An inspection of pipe by snake robot," Int. J. of Advanced Robotic Systems, Vol.13, pp. 1-12, 2016.
[16] H. Shin, K.-M. Jeong, and J.-J. Kwon, "Development of a Snake Robot Moving in a Small Diameter Pipe," Proc. of Int. Conf. on Control, Automation and Systems, October 27-30, 2010 in KINTEX, Gyeonggi-do, Korea, pp. 1826-1829, 2010.
[17] Y. Tanise, K. Taniguchi, S. Yamazaki, M. Kamata, Y. Yamada, and T. Nakamura, "Development of an air duct cleaning robot for housing based on peristaltic crawling motion," Proc. of 2017 IEEE Int. Conf. on Advanced Intelligent Mechatronics (AIM), pp. 1267-1272, 2017.
[18] T. Tomita, T. Tanaka, and T. Nakamura, "Development of a peristaltic crawling robot for long-distance complex line sewer pipe inspections," 2015 IEEE/RSJ Int. Conf. on Intelligent Robots and Systems (IROS), pp. 2742-2747, 2015.
[19] M. Kamata, S. Yamazaki, Y. Tanise, Y. Yamada, and T. Nakamura, "Morphological change in peristaltic crawling motion of a narrow pipe inspection robot inspired by earthworm's locomotion," Advanced Robotics, Vol.32, No.7, pp. 386-397, 2018.
[20] A. Kojima, M. Okui, Y. Yamada, and T. Nakamura, "Prolonging the lifetime of straight-fiber-type pneumatic rubber artificial muscle by shape consideration and material development," Proc. of 2018 IEEE Int. Conf. on Soft Robotics (RoboSoft) Livorno, Italy, pp. 24-28, 2018.
[21] N. Saga, J. Nagase, and T. Saikawa, "Pneumatic artificial muscles based on biomechanical characteristics of human muscles," Applied Bionics and Biomechanics, Vol.3, No.3, pp. 191-197, 2006.

Supporting Online Materials:

[a] Osaka Winton Co., Ltd. http://www.osaka-winton.co.jp/en/air_conditioning/ [Accessed May 11, 2019]

Name:
Fumio Ito

Affiliation:
Master Course Student, Department of Precision Mechanical Engineering, Chuo University

Address:
1-13-27 Kasuga, Bunkyo-ku, Tokyo 112-8551, Japan

Brief Biographical History:
2019- Master Course Student, Department of Precision Mechanical Engineering, Chuo University

Main Works:
• F. Ito, T. Kawaguchi, M. Kamata, Y. Yamada, and T. Nakamura, "Proposal of Bellows Integrated Robot for Improving Flexibility and Sealability of Peristaltic Motion Robot," CLAWAR 2019, 22nd Int. Conf. on Climbing and Walking Robots and the Support Technologies for Mobile Machines, Kuala Lumpur, Malaysia, August 26-28, 2019.

Membership in Academic Societies:
• The Institute of Electrical and Electronics Engineers (IEEE) Robotics and Automation Society (RAS)
• The Japan Fluid Power System Society (JFPS)
• The Japan Society of Mechanical Engineers (JSME)
• The Society of Instrument and Control Engineers (SICE)

Name:
Takahiko Kawaguchi

Affiliation:
Master Course Student, Department of Precision Mechanical Engineering, Chuo University

Address:
1-13-27 Kasuga, Bunkyo-ku, Tokyo 112-8551, Japan

Brief Biographical History:
2018- Master Course Student, Department of Precision Mechanical Engineering, Chuo University

Main Works:
• T. Kawaguchi, Y. Tanise, M. Kamata, Y. Yamada, and T. Nakamura, "Development of a peristaltic crawling motion type duct cleaning robot compatible with cleaning efficiency and running speed by cleaning joint," 21st Int. Conf. on Climbing and Walking Robots and the Support Technologies for Mobile Machines (CLAWAR 2018), Robotics Transforming the Future, 2018.

Name:
Yasuyuki Yamada

Affiliation:
Associate Professor, Faculty of Engineering and Design, Hosei University

Address:
2-33 Ichigayatamachi, Shinjuku-ku, Tokyo 162-0843, Japan

Brief Biographical History:
2011 Received M.S. from Keio University
2013 Received Ph.D. from Keio University
2013-2014 Postdoctoral Researcher, Tokyo Institute of Technology / Keio University
2014-2015 Engineer, Nissan Motor Co., Ltd.
2015-2018 Assistant Professor, Chuo University
2018- Visiting Assistant Professor, Dyson School of Design Engineering, Imperial College London
2019- Associate Professor, Faculty of Engineering and Design, Hosei University

Main Works:
• Y. Yamada, G. Endo, and E. F. Fukushima, "Pneumatic walking assistive device for use over long period," Advanced Robotics, Vol.28, Issue 18, pp. 1253-1264, 2014.
• Y. Yamada, K. Ashigaki, S. Yoshihama, K. Negishi, K. Kato, and T. Nakamura, "Triangular cross section peristaltic conveyor for transporting powders at high speed in printers," Advanced Robotics, Vol.32, Issue 12, pp. 1-13, 2018.
• Paris Fashion Week 2016 AW (YaCHAIKA by ANREALAGE)

Membership in Academic Societies:
• The Institute of Electrical and Electronics Engineers (IEEE) Robotics and Automation Society (RAS)
• The Japan Society of Mechanical Engineers (JSME)
• The Robotics Society of Japan (RSJ)

Name:
Taro Nakamura

Affiliation:
Professor, Faculty of Science and Engineering, Chuo University

Address:
1-13-27 Kasuga, Bunkyo-ku, Tokyo 112-8551, Japan

Brief Biographical History:
1999- Research Associate, Akita Prefectural University
2004- Associate Professor, Department of Precision Mechanics, Chuo University
2012-2013 Visiting Professor, École Polytechnique Fédérale de Lausanne (EPFL)
2013- Professor, Department of Precision Mechanics, Chuo University

Main Works:
• T. Nakamura, Y. Hidaka, M. Yokojima, and K. Adachi, "Development of Peristaltic Crawling Robot with Artificial Rubber Muscles Attached to Large Intestine Endoscope," Advanced Robotics, Vol.26, No.10, pp. 1161-1182, 2012.
• T. Nakamura, M. Maehara, D. Tanaka, and H. Maeda, "Estimation of Joint Stiffness Using Instantaneous Loads via an Electromyogram and Application to a Master-slave System with an Artificial Muscle Manipulator," Advanced Robotics, Vol.26, No.7, pp. 799-816, 2012.
• T. Nakamura and K. Suzuki, "Development of a Peristaltic Pump Based on Bowel Peristalsis using Artificial Rubber Muscle," Advanced Robotics, Vol.25, No.3, pp. 371-385, 2011.
• T. Nakamura and N. Saga, "Viscous Control of Homogeneous ER Fluid Using Variable Structure Control," IEEE/ASME Trans. on Mechatronics, Vol.10, No.2, pp. 154-160, 2005.
• M. Kamata, S. Yamazaki, Y. Tanise, Y. Yamada, and T. Nakamura, "Morphological change in peristaltic crawling motion of a narrow pipe inspection robot inspired by earthworm's locomotion," Advanced Robotics, Vol.32, No.7, pp. 386-397, 2018.

Membership in Academic Societies:
• The Institute of Electrical and Electronics Engineers (IEEE) Robotics and Automation Society (RAS)
• The Japan Society of Mechanical Engineers (JSME)
• The Robotics Society of Japan (RSJ)